Hofmann, W. and Morawska, L. and Winkler-Heil, R. and Moustafa, M. (2009) ***Deposition of combustion aerosols in the human respiratory tract : comparison of theoretical predictions with experimental data***. Inhalation Toxicology, 21(14). pp. 1154-1164.

DEPOSITION OF COMBUSTION AEROSOLS IN THE HUMAN RESPIRATORY TRACT: COMPARISON OF THEORETICAL PREDICTIONS WITH EXPERIMENTAL DATA

W. Hofmann[a], L. Morawska[b], R. Winkler-Heil[a], M. Moustafa[a,c]

[a]Division of Physics and Biophysics, Department of Materials Engineering and Physics, University of Salzburg, Hellbrunner Str. 34, 5020 Salzburg, Austria

[b]International Laboratory for Air Quality and Health, Queensland University of Technology, 2 George Street, Brisbane QLD 4001, Australia

[c]Physics Department, Faculty of Science, El Minia University, El Minia, Egypt

Corresponding author:

Prof. Dr. Werner Hofmann
Division of Physics and Biophysics
Department of Materials Engineering and Physics
University of Salzburg,
Hellbrunner Str. 34
5020 Salzburg, Austria
Tel: ++43-662-8044-5705
Fax: ++43-662-8044-150
E-mail: Werner.Hofmann@sbg.ac.at

Running title: Deposition of combustion aerosols

ABSTRACT

Total deposition of petrol, diesel and environmental tobacco smoke (ETS) aerosols in the human respiratory tract for nasal breathing conditions was computed for 14 nonsmoking volunteers, considering the specific anatomical and respiratory parameters of each volunteer and the specific size distribution for each inhalation experiment. Theoretical predictions were 34.6% for petrol, 24.0% for diesel, and 18.5% for ETS particles. Compared to the experimental results, predicted deposition values were consistently smaller than the measured data (41.4% for petrol, 29.6% for diesel, and 36.2% for ETS particles). The apparent discrepancy between experimental data on total deposition and modeling results may be reconciled by considering the non-spherical shape of the test aerosols by diameter-dependent dynamic shape factors to account for differences between mobility-equivalent and volume-equivalent or thermodynamic diameters. While the application of dynamic shape factors is able to explain the observed differences for petrol and diesel particles, additional mechanisms may be required for ETS particle deposition, such as the size reduction upon inspiration by evaporation of volatile compounds and/or condensation-induced restructuring, and, possibly, electrical charge effects.

INTRODUCTION

A previous comparison between experimental and theoretical total deposition data for environmental tobacco smoke (ETS) with count median diameter (CMD) of 0.2 μm revealed a significant discrepancy between experiment and theory. While a total deposition of 56% was observed for nasal breathing conditions in 15 nonsmokers (Morawska et al., 1999), stochastic model calculations predicted a value of only 17% (Hofmann et al., 2001). If, however, that same stochastic deposition model (Hofmann & Koblinger, 1990; Koblinger & Hofmann, 1990) was applied to the inhalation of monodisperse, spherical particles in the size range of the ETS particles (Heyder et al., 1986; Schiller et al., 1986, 1988), excellent agreement was found between theoretical predictions based on the stochastic model and corresponding experimental data on total and regional deposition in human test subjects for a wide range of particle sizes and breathing patterns (Hofmann & Koblinger, 1990, 1992; Bergmann et al., 1997). This suggests that additional mechanisms must be considered in the case of polydisperse, non-spherical combustion aerosols, particularly for ETS. Potential factors discussed in a previous analysis were hygroscopic growth, coagulation, electrical charge, and cloud settling (Hofmann et al., 2001). It was then concluded that only a combination of all these factors, if at all, may be necessary to reconcile experimental and theoretical deposition data.

To further investigate this discrepancy, which may be specific to polydisperse, non-spherical combustion aerosols, additional measurements were carried out for petrol, diesel, and ETS aerosols, ranging in size from 40 to 220 nm (Morawska et al., 2005). Thus the objectives of this theoretical analysis were (i) to compare the new experimental data with model predictions, and (ii) in case of still existing differences, to explore additional mechanisms, which may explain that discrepancy.

COMPUTATIONAL MODEL

Deposition model

Total deposition of inhaled petrol, diesel and ETS particles was calculated using an updated version of the Monte Carlo transport and deposition code IDEAL (Hofmann & Koblinger, 1990; Koblinger & Hofmann, 1990), which is based on a stochastic morphometric model of the human lung (Koblinger & Hofmann, 1985). The stochastic asymmetric morphometric model describes the inherent asymmetry and variability of the human airway system in terms of probability density functions of airway diameters, lengths and branching angles and correlations among some of the morphometric parameters. The dimensional and structural parameters of this model were derived from morphometric measurements of the trachebronchial tree of two human subjects (Raabe et al., 1976) and from a morphometric analysis of several acini of the human alveolar region (Haefeli-Bleuer & Weibel, 1988). As the measured bronchial airway dimensions reportedly refer to total lung capacity (Schum & Yeh, 1980), all bronchial airway diameters and lengths were isotropically scaled down to a functional residual capacity (FRC) of 3300 ml (ICRP, 1994) by a constant linear scaling factor. Upon inspiration, each airway is assumed to expand at the same rate and thus airway diameters and lengths at a given tidal volume (V_T) are finally rescaled to a total lung volume of FRC + V_T/2.

In the Monte Carlo transport and deposition model, the random walk of inspired particles through a stochastically generated airway branching system is simulated by randomly selecting a sequence of airways for each individual particle. The random selection of the linear airway dimensions of both daughter airways at each bifurcation is based on the probability density functions of geometric airway parameters, e.g. airway diameters, constrained, however, by correlations among some of these parameters, e.g. between cross sections of major and minor daughters or between airway diameters and branching angles

(Koblinger & Hofmann, 1985). The actual path of the inhaled particle into either the major or minor daughter branch is then randomly selected from the airflow distribution, assuming that flow splitting is proportional to distal volume (Phillips & Kaye, 1997). The penetration of inhaled particles into the lungs is determined by the time of inspiration during the inspiration period, which is randomly selected for each particle from a uniform time distribution. In case of a deposition event, which would also terminate the path of an inhaled particle, deposition of a particle in a given airway is simulated by decreasing its statistical weight, i.e., the particle continues its path with a smaller statistical weight. The contribution of a deposition event to deposition in a given airway is then determined by the product of the actual statistical weight times the deposition probability in that airway.

Particle deposition in individual airways due to the various physical deposition mechanisms was computed by the commonly used analytical deposition equations for straight and bent tubes, i.e., deposition of an individual particle is based on the average deposition behavior of many particles. The filtering efficiency of nasal passages for submicron particles was considered by empirical equations derived from in vivo measurements (Cheng et al., 1996). Deposition by Brownian motion in upper bronchial airways was determined by the empirical equation proposed by Cohen & Asgharian (1990) to account for enhanced deposition due to developing flow. Outside the range of flow rates and airway dimensions of this relationship, i.e., in more peripheral airways, Ingham's (1975) equation for diffusion deposition under parabolic flow conditions was applied. Axial diffusion is modeled by an effective axial diffusivity, which depends on particle size (diffusion coefficient) and airway generation (flow velocity and airway diameter), modified by results of numerical simulations of bolus dispersion in multiple airway bifurcation models (Hofmann et al., 2003). The magnitude of deposition by inertial impaction in upper bronchial airways was calculated according to Yeh & Schum (1980).

To demonstrate the validity of the stochastic deposition model for ultrafine particles, predicted total deposition values were compared in Figure 1 with the experimental data of Schiller et al. (1988). Considering the effect of intersubject variability on lung deposition, excellent agreement between experimental data and theoretical predictions could be obtained, especially for the size range (40 - 200 nm) and the breathing parameters (V_T = 670 ml, f = 16 min^{-1}) employed in the combustion aerosol inhalation experiments (Morawska et al., 2005).

This model, validated by comparison with experimental data for monodisperse, spherical particles, was applied here to experimental data for polydisperse, non-spherical particles. Since the equations used in the standard model for diffusional and inertial particle deposition efficiencies refer to spherical particles and combustion aerosols are chain-like aggregates, the modifications of the diffusion coefficient and the Stokes number for random orientation proposed by Asgharian & Yu (1990) were applied. The additional effect of direct interception at the carina of airway bifurcations (Yu & Xu, 1986; Asgharian & Yu, 1989, 1990), which may play a role for elongated particles, was modeled by the equation proposed by Asgharian & Yu (1990) for random orientation.

Anatomical and respiratory parameters of volunteers in the experimental study

For inhalation risk assessment purposes, ICRP (1994) proposes the following standard respiratory parameters under sitting breathing conditions for adult males and females with a standard functional residual capacity, FRC, of 3300 ml: tidal volume V_T = 0.75 l (male) and 0.464 l (female), and breathing frequency f = 12 min^{-1} (male) and 14 min^{-1} (female). In order to investigate the effect of intersubject variations of anatomical (FRC) and respiratory parameters (V_T, f) on particle deposition, the 14 test persons between the ages of 20 and 30 aking part in the inhalation experiments (Morawska et al., 2005) participated also in pulmonary function tests. While breathing frequencies were directly measured, corresponding

tidal volumes were derived from measured vital capacity (VC) values by assuming a constant empirical ratio between V_T and VC (ICRP 1994). The FRC values for each volunteer were obtained from empirical relationships between FRC and age and height of females and males (ICRP, 1994). The derived data were consistent with the assumption of a constant relationship between FRC and VC (ICRP, 1994).

The individual anatomical and respiratory parameters of the 14 volunteers are compiled in Table 1, displaying a wide range of intersubject variations in breathing patterns and lung volumes. Compared to the standard values proposed by ICRP (1994), the average FRC of 3080 ml is slightly smaller than the ICRP value of 3300 ml, while tidal volumes and breathing frequencies are consistently higher than the standard values. The latter suggests that breathing during a pulmonary function test or breathing through a mask during the experiment seems to induce some stress in a volunteer (Askanazi et al., 1980).

For the calculation of individual total deposition fractions, airway dimensions in each volunteer were scaled in proportion to the cube root of the FRC, relative to the standard FRC of 3300 ml. Furthermore, individual inspiration and expiration times were derived from the measured breathing frequencies, assuming equal inspiration and expiration phases without pause.

MODEL PREDICTIONS AND COMPARISON WITH EXPERIMENTAL DATA

Deposition of environmental tobacco smoke (ETS), diesel and petrol smoke aerosols in the human respiratory tract was determined experimentally in 14 non-smoking test persons. Scanning Mobility Particle Sizer (SMPS) was used to characterize the inhaled and exhaled aerosol size distributions in the size range of 16 – 626 nm during relaxed breathing over a period of 10 minutes. The ETS, diesel and petrol particles had count median diameters (and

geometric standard deviations) of 184 nm (1.7), 125 nm (1.7) and 69 nm (1.7), respectively. For a detailed description of the experimental procedures, the reader is referred to the original article of Morawska et al. (2005).

Total deposition

Total deposition for nasal breathing conditions was computed for each experiment, considering the specific anatomical (FRC) and respiratory parameters (V_T, f) of each volunteer, listed in Table 1, and the specific particle size distributions for each aerosol and volunteer, listed in Table 2. Predicted total deposition fractions, considering the combined effect of intersubject variations in physiological parameters and particle size distribution, are also listed in Table 2 for all three test aerosols. Consistent with the dependence of diffusion deposition on particle diameter, predicted total deposition decreases with increasing CMD of the inhaled aerosol.

The effect of different modeling assumptions on total particle deposition is shown in Table 3, varying particle (monodisperse vs. polydisperse and average CMD vs. individual CMD) as well as breathing parameters (standard vs. individual breathing). While the use of individual data instead of standard or average values hardly affects total deposition, consideration of polydispersity significantly decreases deposition relative to the corresponding monodisperse averages as a result of the lognormal shape of the size distributions.

Experimental total deposition data for each volunteer inhaling the three aerosols are plotted in Figure 2. Due to differences in particle size and respiratory parameters, total deposition data for each inhalation experiment varied considerably.

Each of the three test aerosols exhibits a considerable range of CMDs. For ETS, the CMD had a standard deviation of 0.030 μm, for diesel it was 0.025 μm and for petrol 0.017 μm. This variability of the aerosol spectrum was caused by uncontrollable differences of specific

sampling and exposure conditions (Morawska et al., 2005). These variations in CMDs, however, would non affect the deposition data obtained in this study because each aerosol had only little variation with respect to both concentration and size distribution throughout each individual subject's test. Intersubject variations of lung volumes (FRC) and breathing parameters (V_T, f) as listed in Table 1 will further increase the variations observed for total deposition.

Average measured and predicted total deposition data for the 3 test aerosols are summarized in Figure 3, assuming that the particle diameter recorded by the SMPS represents the thermodynamic (or geometric) diameter used for the calculation of the diffusion coefficient in the theoretical predictions. The average measured total deposition of ETS was 36.2 ± 10%, of diesel smoke 29.6 ± 9%, and of petrol smoke 41.4 ± 8%. To illustrate the dependence of total deposition on particle diameter, deposition was also calculated for a standard FRC of 3300 ml and sitting breathing conditions for an adult male (ICRP, 1994). Despite the validation of the deposition model by comparison with monodisperse, spherical particles (see Figure 1), predicted total deposition is still consistently lower than the corresponding experimental results for all three aerosols, particularly for the ETS particles.

Theoretical predictions are compared in Table 4 with the measured total deposition values for male and female volunteers. For all three aerosols, computed deposition is significantly smaller than the corresponding measured data, the greatest difference occurring for the ETS particles. Consistent with diffusion theory and experimental data for monodisperse, spherical particles, total deposition should decrease with increasing particle size. While this is true for petrol and diesel particles, experimental deposition for ETS particles increases again relative to diesel aerosols despite their larger particle size. While this suggests that ETS aerosols may have some unique properties, which cause the observed deviation, it must also be noted that in the narrow size range where diesel and ETS aerosols overlap, both data groups show similar

values. Furthermore, the model correctly predicts a consistently higher deposition in males than in females, which is also borne out by the measurements.

Fractional deposition

As displayed in Figure 2, the CMDs of a given test aerosol varied over a relatively wide range among the 14 volunteers. For example, the smallest CMD for diesel particles was 87 nm, while the largest value was 187 nm. Since the deposition efficiency nearly drops by a factor of about two from 87 to 187 nm, the average CMDs for a given test aerosol plotted in Figure 3 may not correctly represent the dependence of total deposition on particle diameter.

Hence fractional deposition, i.e. deposition fractions in each of the SMPS size bins, was determined for each subject and aerosol (Morawska et al., 2005), indicating significant intersubject variations. Measured average fractional depositions of all subjects for each of the three aerosols are plotted in Figure 4 as a function of the thermodynamic (or geometric) particle diameter, together with the theoretical curve for monodisperse, spherical particles using the average breathing conditions of the volunteers (Table 1). While theoretical deposition, consistent with experimental data for spherical particles (ICRP, 1994) decreases with increasing particle diameter in the diffusion-dominated size range, this decline is less significant for the diesel and petrol aerosols, and practically absent for the ETS particles.

EFFECT OF PARTICLE SHAPE ON DEPOSITION

The above comparison between experimental data and theoretical predictions for the three test aerosols reveals two significant differences: (i) measured total deposition values are consistently higher than those predicted by the model, and (ii) the dependence of measured fractional deposition on particle diameter is not consistent with diffusion theory, particularly for ETS particles. Since model predictions exhibit excellent agreement with experimental data

for spherical particles, these differences may be attributed to the non-spherical shape of the inhaled test aerosols. Hence the role of particle shape on deposition will be investigated in more detail.

The non-spherical shape of the test aerosols affects measured size distributions as well as particle deposition calculations. In case of spherical particles, the mobility equivalent diameter, obtained in the measurements, and the thermodynamic (or geometric) diameter, used for the calculation of the diffusion coefficient by the Stokes-Einstein equation, have the same numerical value. Indeed, the deposition measurements of Schiller et al. (1988) with monodisperse, spherical, hydrophobic, uncharged silver particles in a diffusion battery demonstrated that electrical mobility-equivalent diameters agreed with diffusion-equivalent or thermodynamic diameters. However, in case of non-spherical, fractal-like particles used in the present study, the drag force experienced by an irregularly shaped particle is higher than that for a spherical particle having the same volume. According to Kasper (1982), the mobility-equivalent particle diameter of a non-spherical particle, d_{me}, can be related to the volume-equivalent diameter of a spherical particle, d_{ve}, by a dynamic shape factor, χ, to give the same drag force:

$$d_{me} = \chi \, d_{ve} \, C_{me} / C_{ve} \qquad (1)$$

where C_{ve} and C_{me} are the related Cunnigham slip correction factors.

Typical values of χ lie in the range of 1 to 2, e.g. $\chi = 1.95$ for coal dust (Hinds, 1999), or $\chi = 1.54$ for a prolate ellipsoid with an axis ratio of 0.1 (Friedlander, 2000). Dynamic shape factors of soot aggregates from wood combustion were between 1.5 and 2.5, increasing with rising number of primary particles (Gwaze et al., 2006). Park et al. (2004) found that the dynamic shape factor increased from 1.11 to 2.21 as the diameter of diesel exhaust particles increased from 50 to 220 nm.

In terms of the diffusion coefficient for the deposition calculations, this relationship leads to

$$D_{me} = D_{ve} \; C_{ve} / \chi \, C_{me} \qquad (2)$$

where D_{me} is the diffusion coefficient for the non-spherical particle and D_{ve} the diffusion coefficient of the volume- equivalent diameter for a spherical particle. Thus, if experimental and theoretical deposition is expressed in terms of the volume-equivalent particle diameter, then the experimental deposition values for the three test aerosols will be shifted to smaller particle sizes, more in line with the model predictions. Alternatively, if experimental and theoretical deposition is expressed in terms of the measured mobility-equivalent particle diameter, then the computed deposition values for the three test aerosols will be shifted to larger particle diameters.

In Figure 3, total deposition is plotted as a function of the thermodynamic particle diameter of unit density spherical particles to facilitate comparison with commonly used monodisperse, spherical particles. Thus to relate the measured mobility-equivalent diameters of the three aerosols to their corresponding volume-equivalent or thermodynamic diameters, they have to be divided by their dynamic shape factors (eq. 1).

Empirical average dynamic shape factors, defined as the ratio of the CMDs measured in the experiments divided by the CMDs of the reduced hypothetical size distributions to match the corresponding experimental values, are listed in Table 5. These numerical values for the dynamic shape factors must be interpreted as average values for the whole size spectrum, i.e. related to the average CMD for each test aerosol. The required dynamic shape factors of 1.21 for petrol and of 1.59 for diesel aerosols lie indeed within the range of reported values. Although dynamic shape factors were not measured at the time of the inhalation experiments, the application of published dynamic shape factors for petrol and diesel may reconcile the experimental and theoretical deposition data for the two aerosols. The difference in the

dynamic shape factors may be attributed to morphological differences of the two types of combustion aerosols, as diesel particles consist mainly of chain aggregates, while petrol particles contain a substantial amount of volatile material and thus a more spherical (Wang & Friedlander, 2007). For the ETS particles, however, the dynamic shape factors proposed for the petrol and diesel aerosols are too small to explain an empirical shape factor of 2.69.

To investigate the effect of shape factors and their related deposition patterns on the exhaled particle sizes, expiratory particle size spectra were calculated for the average inhaled size spectra of the three test aerosols (Morawska et al. 2005), varying the shape factors within the above range of values. If no shape factor is considered at all, i.e. $\chi = 1$, the CMDs of all three aerosols are shifted slightly to higher values, e.g. from 184 nm to 191 nm for ETS particles, as the particles with diameters less than the medians are preferentially deposited relative to those with larger diameters of the lognormal size distributions. However, an increase of the shape factor in the range from 1 to 2 did not change the CMDs in the exhaled air. Thus the observation that CMDs in inhaled and exhaled air are practically the same within the experimental error is consistent with the application of dynamic shape factors in this range.

While the shift of the experimental results to smaller sizes reduces and possibly even eliminates the differences between experimental data and theoretical predictions, the application of such average dynamic shape factors still cannot explain the relative insensitivity to particle size in the diffusion domain as exhibited in the fractional deposition data, particularly for the ETS particles. This discrepancy can only be reconciled by assuming that dynamic shape factors for the three aerosols are functions of the particle diameter, where larger diameter aerosols have higher shape factors, and vice versa. Indeed, Park et al. (2004) found that the dynamic shape factor increased from 1.11 to 2.21 as the mobility diameter of diesel exhaust particles increased from 50 to 220 nm. They attributed this increase in dynamic

shape factor to the increasing irregularity of diesel particles with size, i.e. larger particles are more irregular than smaller ones. For even higher mobility diameters, between 100 and 400 nm, Slowik et al. (2004) reported that dynamic shape factors further increased in a nearly linear fashion up to a value of about 3. Both data sets for diesel particles were fitted by a polynomial function and extrapolated to 600 nm to cover the whole range of particle diameters used in this study (Figure 5).

The effect of this dynamic shape factor function, based on the experimental data of Park et al. (2004) and Slowik et al. (2004), on total deposition is illustrated in Figure 3 for all three test aerosols. For the deposition calculations, average mobility-equivalent diameters were converted to average volume-equivalent diameters by weighting the measured size distributions by the dynamic shape factor function. Considering the effect of intersubject variability in the total and fractional deposition data and potential differences in particle morphology, and thus shape factor, surprisingly good agreement could be obtained for the petrol and diesel aerosols. The differences between petrol and diesel particles in the dynamic shape factor values are consistent with the reported increase of the shape factor with growing diameter. This agreement indicates that the differences between experimental data and theoretical predictions of fractional deposition data are indeed caused by the non-spherical shape of the combustion particles. It further suggests that the dynamic shape factor concept is an appropriate method to characterize the deposition behavior of fractal combustion aggregates.

DEPOSITION OF ETS PARTICLES

While the assumption of diameter-dependent shape factors explains satisfactorily the deviation from diffusion theory for the petrol and diesel particles, problems still exist for the ETS particles, where fractional deposition is relatively insensitive to particle size over the

measured size range. Thus one possible explanation is that dynamic shape factors for ETS particles are either generally higher than for diesel particles and/or that they further increase beyond the 50 - 400 nm range reported by Park et al. (2004) and Slowik et al. (2004). The latter hypothesis would be consistent with the finding of Park et al. (2004) who attributed the increase in dynamic shape factor to the increasing irregularity of diesel particles with size, i.e. larger particles are more irregular than smaller ones. However, extrapolating the dynamic shape factor function measured by Slowik et al. (2004) up to 600 nm (see Figure 5) only slightly reduces the differences between experiment and modeling. Only the assumption of a dynamic shape factor increasing linearly to an unrealistically high value of about 9 at 600 nm would produce the desired effect. Thus dynamic shape factors for ETS particles either generally adopt higher values than for diesel aerosols or additional physical mechanisms may play a role.

Mechanisms affecting particle size

The first group of mechanisms includes those which affect particle size upon inspiration, such as increase in size due to hygroscopic growth or coagulation, or size reduction by evaporation of volatile compounds and/or condensation-induced restructuring or increase in size due to hygroscopic growth or coagulation.

Comprehensive characterization of hygroscopic growth of fresh and aged ETS was previously reported by Morawska et al. (1998), suggesting that hygroscopic growth of ETS in the lungs may be of the order of 20 - 30%. Alternatively, hygroscopic growth in nasal passages may reduce nasal deposition so that more particles can reach the lungs, thereby increasing total deposition. Implementation of the algorithm developed by Schroeter et al. (2001) for the effect of hygrosopic growth on ETS in human nasal passages into the stochastic deposition model, nasal deposition efficiencies for 183 nm CMD ETS particles were reduced

by hygroscopic growth from 1.44% to 1.16%. These calculations are based on the assumption that growth is completed within the nasal airways for the flow and particle sizes employed in this study, eventually reaching a maximum hygroscopic growth factor of 1.8. Assuming the same growth conditions for petrol and diesel particles, corresponding deposition efficiencies were 0.46% vs. 0.39% (69 nm CMD), and 0.78% vs. 0.58% (124 nm CMD). This indicates that nasal deposition hardly affects the number of particles entering the lung and hence total deposition. Since the size spectra of the particles exiting the nasopharyngeal region are shifted to larger particle diameters by a factor of 1.8, hygroscopic growth leads to a reduction of particle deposition in the thoracic region, and, consequently, to total deposition. In the case of ETS particles, total deposition is reduced from 16.5% to 13.8%. Thus hygroscopic growth would actually widen the gap between experimental and theoretical results rather than reducing it. In conclusion, hygroscopic growth may not appreciably affect total deposition in the present study.

Coagulation is well known as another mechanism, which may increase particle size upon inspiration (Robinson & Yu, 1999, 2001). For example, modeling coagulation of cigarette smoke as a polydisperse-charged aerosol, numerical results indicated that the size distribution of sidestream cigarette smoke, with a concentration of 10^6 particles per cm^3, remains practically unchanged for 2 seconds (Robinson & Yu, 1999). Since the particle concentrations in the present experiments (Morawska et al., 2005) were about 5×10^{-4} cm^{-3} and thus well below the region where coagulation will play a role, this effect may safely be neglected in the present analysis. Moreover, a potential effect of coagulation would further decrease the theoretical predictions for the three test aerosols rather than to elevate them to the level of the experimental values.

While hygroscopic aerosol particles grow in size by hygroscopic growth, the size of a non-hygroscopic particle may also decrease by evaporation of volatile substances. If a particle

consists of an involatile hard core and a volatile outer shell, then the sudden temperature rise upon inhalation may induce evaporation of the volatile compounds in the outer shell of the particles, thereby reducing particle size and, consequently, increasing deposition (Müller, 2000, 2004). Moreover, with rising temperature, semivolatile species escape into the gas phase, thereby further enhancing the evaporation effect. Based on the equations proposed by Müller (2000, 2004) on the dependence of the mass median diameter (MMD) and the gaseous fraction on vapor pressure and temperature, size reduction factors for non-hygroscopic particles range from about 1.1 to 1.7 for various inorganic and organic substances. Indeed, a diameter reduction factor of 1.7, assumed in addition to the dynamic shape factor effect shown in Figure 5, would reconcile experiment with modelling. Thus, such evaporation effects may contribute to the experimentally observed higher deposition values of ETS particles in addition to non-spherical particle effects. In case of partly hygroscopic particles, this diameter reduction may be compensated to some degree by hygroscopic growth.

An alternative explanation for the shrinking of particles during inhalation is offered by Kűtz & Schmidt-Ott (2004) through condensation-induced restructuring of agglomerates of primary particles in the humid atmosphere of the lungs. At a certain degree of evaporation, the primary particles tend to deform the droplet, while surface tension tries to retain the spherical shape, thereby reducing the diameter of the droplet. While this effect may be less significant for aerosols with a rather stable inner structure, e.g. diesel and petrol aerosols, more loosely structured aerosols, such as ETS particles, may collapse more readily to a rather spherical shape due to capillary forces. Thus the additional effect of capillary condensation may explain why the difference between measured and calculated particle deposition is most pronounced for ETS particles. Again, a diameter reduction factor of 1.7 for ETS particles would be needed to reconcile experimental with predicted total deposition.

Additional deposition mechanisms

The second group of mechanisms comprises additional physical deposition mechanisms presumed to be effective for mainstream cigarette smoke deposition. These mechanisms may have to be considered for ETS deposition as well, such as the effect of electrical charge effects or cloud behavior. The stochastic deposition model used for the present calculations considers the effects of deposition by Brownian motion, inertial impaction and gravitational settling. Thus a possible reason for predicting lower total deposition than found in the experiments could also be that additional mechanisms, such as electrical charge effects or cloud settling, must be included.

Due to the relatively small particle concentrations used in this study, only image forces, i.e., the electrostatic interaction between particles and the conducting surface of the airway walls, must be considered. Measurements of the charge status of mainstream cigarette smoke and vehicle exhaust particles have shown that large fractions of particles, approximately 60-80% are electrically charged, exhibiting a symmetric charge distribution with a charge per particle of about one or two, which leaves the combustion aerosols essentially electrically neutral (Robinson & Yu, 1999; Park et al., 2004; Maricq, 2006). Measurements in human test subjects have demonstrated that total deposition of particles in the range of 0.3 - 1.0 μm increases with increasing charge for highly charged aerosols (Melandri et al., 1983), say above about 30 electrostatic charge units (Yu, 1985), which is far above the measured charge values. However, Cohen et al. (1998) showed that even singly charged ultrafine particles in hollow-cast models of human airways may considerably increase deposition in upper bronchial airways. In the present study, a deposition enhancement factor of 1.5 would be needed to achieve agreement between experiment and calculations, which lies well in the range of the values reported by Cohen at al. (1988). Since no charge measurements were

made in the experimental study, it is presently not possible to estimate the effect of electrical charge on the deposition of the three test aerosols.

Cloud settling or colligative behavior would increase deposition of concentrated inhaled particles, such as in mainstream cigarette smoke, by impaction, sedimentation and interception (Broday & Robinson, 2003; Martonen, 1992; Martonen & Musante, 2000; Robinson & Yu, 2001). However, for particle concentrations of 5 x 10^{-4} cm^{-3} used in the experiments (Morawska et al., 2005), individual particle motion should prevail and no cloud motion effect should be observed (Martonen, 1992).

DISCUSSION

Although the above discussed effects seem to reconcile most of the observed discrepancy between experimental and theoretical deposition data, other factors may also play a role. For example, the anatomical (FRC) and physiological parameters (V_T, f) used in the calculations may be different from those during the in vivo inhalation studies. Since the FRC and V_T values for each volunteer were derived from empirical equations (ICRP, 1994), the question arises whether these empirical relationships, describing the average behavior of many individuals, also holds for a given individual. Thus the FRC of each volunteer was varied by ± 16%, as suggested by the statistical uncertainties of the equations, to simulate the potential effect of FRC variations on total deposition. The resulting uncertainties in total deposition suggest that any errors in the FRC calculations would not appreciably affect the deposition results. For example, a decrease of FRC by 16% would increase total deposition by only about 1%. Calculations for V_T variations give similar results, with total deposition slightly decreasing for higher tidal volumes.

Although breathing frequencies measured at the time of the test were generally similar to those obtained during the pulmonary function tests (which were eventually used for the

deposition calculations), there were a few volunteers whose breathing frequencies were consistently smaller during the inhalation experiment. To simulate the potential effect of a slower breathing at the time of the inhalation experiment on particle deposition, breathing frequencies were reduced by 20% as suggested by the measured data. As expected for particles in the diffusion domain, this decrease in breathing frequency increases average total deposition by about 2% for all three aerosols. Thus the assumption of a slower breathing during the experiment increases total deposition, but would only slightly reduce the observed discrepancy between experimental and theoretical data. In conclusion, any potential errors in the determination of anatomical and physiological input parameters do not appreciably affect total deposition calculations.

The quantification of the non-spherical shape of combustion aerosols in terms of dynamic shape factors is able to explain the observed differences between measured and predicted total deposition for petrol and diesel particles. This apparent discrepancy was primarily caused by using mobility-equivalent diameters for reporting the measurements and volume-equivalent diameters for the determination of diffusion coefficients used in the deposition calculations. Indeed, Wang and Friedlander (2007) recently concluded that the total deposition data of Morawska et al. (2005) for diesel and petrol exhaust particles agree well with predicted deposition fractions when measured particle diameters are expressed as diffusion-equivalent diameters. Thus measurements of the size distribution of non-spherical particles must include some estimates of the dynamic shape factor. Otherwise, deposition estimated on the basis of models using spherical particles will underestimate deposition and thus risk. An alternative method to directly measure the effect of non-spherical shape is the derivation of effective densities through the combined measurement of the mobility-equivalent diameters and aerodynamic-equivalent diameters (Park et al., 2003; Schmid et al., 2007).

In conclusion, the observed discrepancy between measured and predicted total deposition for diesel and petrol aerosols can be reconciled by the application of dynamic shape factors. Their measured dependence on particle diameter can also explain the relative insensitivity of their fractional deposition to particle diameter variations. In the case of ETS particles, additional factors may have to be incorporated into current deposition models. Estimates of the magnitudes of the potential effects of non-spherical shape, evaporation, condensation-induced restructuring, and electrical charges on total and fractional deposition suggest that a combination of several of these mechanisms may be necessary to reconcile ETS experimental and theoretical deposition data, the most likely candidates being non-spherical shape, evaporation and capillary condensation, and, possibly, charge effects. However, in case the ETS inhalation experiments (Morawska et al., 2005), the time between the production and inhalation of ETS particles may have been long enough so that evaporation as well as uptake of water molecules have already partly taken place before inhalation, thereby diminishing the effects of non-spherical shape, evaporation and condensation-induced restructuring. These additional factors may also contribute to petrol and diesel deposition, but their relative magnitudes are most likely much smaller than the effect of the dynamic shape factor. Since quantitative information on the relative magnitudes of these mechanisms for the three test aerosols used in the present study is only partly available at present, only additional experiments can clarify these issues.

ACKNOWLEDGEMENTS

This research was supported in part by the European Communities, Contract No. FIGD-CT-2000-00053, the Austrian Exchange Service, Department of Development Cooperation, Project No. 894/01 (M. Ahmed), and the ARC Linkage International Grant no. LX0445294.

REFERENCES

Asgharian, B., and Yu, C.P. 1989. A simplified model of interceptional deposition of fibers at airway bifurcations. *Aerosol Sci. Technol.* 11:80-88.

Asgharian, B., and Yu, C.P. 1990. Deposition of straight chain aggregates in the human lung. *Aerosol Sci. Technol.* 12, 777-785.

Askanazi, J., Silverberg, P.A., Foster, R.J., Hyman, A.I., Milic-Emili, J., and Kinney, J.M. 1980. Effects of respiratory apparatus on breathing pattern. *J. Appl. Physiol.* 48:577- 580.

Bergmann, R, Hofmann, W., and Koblinger, L. 1997. Particle deposition models in the human lung: Comparison between Monte Carlo and ICRP model predictions. *J. Aerosol Sci.* 28, Suppl. 1: S433-S434.

Broday, D.M., and Robinson, R. 2003. Application of cloud dynamics to dosimetry of cigarette smoke particles in the lungs. *Aerosol Sci. Technol*. 37:510-527.

Cheng, K.H., Cheng, Y.S., Yeh, H.C., Guilmette, R.A., Simpson, S.Q., Yang, Y., and Swift, D.L. 1996. *In vivo* measurements of nasal airway dimensions and ultrafine aerosol deposition in the human nasal and oral airways. *J. Aerosol Sci.* 27:785-801.

Cohen, B.S., and Asgharian, B. 1990. Deposition of ultrafine particles in upper airways. *J. Aerosol Sci.* 21:789-797.

Cohen, B.S., Xiong, J.Q., Fang, C.P., and Lei, W. 1998. Deposition of charged particles on lung airways. *Health Phys.* 74:554-560.

Friedlander, S.K. 2000. *Smoke, dust, and haze*. New York: Oxford University Press.

Gwaze, P., Schmid, O., Annegarn, H.J., Andreae, M.O., Huth, J., and Helas, G. 2006. Comparison of three methods of fractal analysis applied to soot aggregates from wood combustion. *J. Aerosol Sci*. 37:820-838.

Haefeli-Bleuer, B., and Weibel, E.R. 1988. Morphometry of the human pulmonary acinus. *Anat. Rec.* 220:401-414.

Heyder, J., Gebhart, J., Rudolf, G., Schiller, C.F., and Stahlhofen, W. 1986. Deposition of particles in the human respiratory tract in the size range 0.005 – 15 μm. *J. Aerosol Sci.* 17: 811-825.

Hinds, W.C. 1999. *Aerosol technology – properties, behavior, and measurement of airborne particles*. New York: John Wiley & Sons.

Hofmann, W.,and Koblinger, L. 1990. Monte Carlo modeling of aerosol deposition in human lungs. Part II: Deposition fractions and their parameter variations. *J. Aerosol Sci.* 21:675-688.

Hofmann, W., and Koblinger, L. 1992. Monte Carlo modeling of aerosol deposition in human lungs. Part III: Comparison with experimental data. *J. Aerosol Sci.* 23:51-63.

Hofmann, W., Morawska, L., and Bergmann, R. 2001. Environmental tobacco smoke deposition in the human respiratory tract: Differences between experimental and theoretical approaches.

J. Aerosol Med. 14:317-326.

Hofmann, W., Sturm, R., Winkler-Heil, R., and Pawlak, E. 2003. Stochastic model of ultrafine particle deposition and clearance in the human respiratory tract. *Radiat. Prot. Dosim.* 105:77-80.

Ingham, D.B. 1975. Diffusion of aerosol from a stream flowing through a cylindrical tube. *J. Aerosol Sci.* 6:125-132.

International Commission on Radiological Protection (ICRP). 1994. *Human respiratory tract model for radiological protection*. ICRP Publication 66. Oxford: Pergamon Press.

Kasper, G. 1982. Dynamics and measurements of smokes. I. Size characterization of nonspherical particles. *Aerosol Sci. Technol.* 1:187-199.

Koblinger, L., and Hofmann, W. 1985. Analysis of human lung morphometric data for stochastic aerosol deposition calculations. *Phys. Medicine Biol.* 30:541-556.

Koblinger, L., and Hofmann, W. 1990. Monte Carlo modeling of aerosol deposition in human lungs. Part I: Simulation of particle transport in a stochastic lung structure. *J. Aerosol Sci.* 21:661-674.

Kűtz, S., and Schmidt-Ott, A. 1992. Characterization of agglomerates by condensation-induced restructuring. *J. Aerosol Sci.* 23, Suppl. 1: S357-S360.

Maricq, M.M. 2006. On the electrical charge of motor vehicle exhaust particles. *J. Aerosol. Sci*. 37:858-874.

Martonen, T.B. 1992. Deposition patterns of cigarette smoke in human airways. *Am. Ind. Hyg. Assoc. J.* 53:6-18.

Martonen, T.B., and Musante, C.J. 2000. Importance of cloud motion of cigarette smoke deposition in the lung. *Inhal. Toxicol*. 12 (Suppl. 4):261-280.

Melandri, C., Tarroni, G., Prodi, V., De Zaiacomo, T., Formignani, M., and Lombardi, C. 1983. Deposition of charged particles in the human airways. *J. Aerosol Sci.* 14:657-669.

Morawska, L., Barron, W., Hitchins, J., and Ristovsky, Z. 1998. The hygroscopic growth of polydisperse salt, organic and environmental tobacco smoke aerosols for different residence times. *J. Aerosol Sci.* 29, Suppl. 1: S279-S280.

Morawska, L., Barron, W., and Hitchins, J. 1999. Experimental deposition of environmental tobacco smoke submicrometer particulate matter in the human respiratory tract. *Am. Ind. Hyg. Assoc. J.* 60:334-339.

Morawska, L., Hofmann, W., Hitchins-Loveday, J., Swanson, C., and Mengersen, K. 2005. Experimental study of the deposition of combustion aerosols in the human respiratory tract. *J. Aerosol Sci.* 36:939-957.

Müller, J. 2000. Growth and diminuation of aerosol particles. In *Aerosols and health*, pp. **xxx-xxx**. Kernforschungszentrum Karlsruhe (KFK) Report U113. Karlsruhe, Germany.

Müller, J. 2004. Mass median diameter (MMD) of aerosol substances in dependence of temperature. In *European Aerosol Conference 2004,* Book of Abstracts, pp. S237-S238. Budapest, Hungary.

Park, K., Cao, F., Kittelson, D.B, and McMurray, P.H. 2003. Relationship between particle mass and mobility for diesel exhaust particles. *Environ. Sci. Technol*. 37:577-583.

Park, K., Kittelson, D.B., and McMurray, P.H. 2004. Structural properties of diesel exhaust particles measured by transmission electron microscopy (TEM): Relationship to particle mass and mobility. *Aerosol Sci. Technol.* 38:881-889.

Phillips, C.G., and Kaye, S.R. 1997. On the asymmetry of bifurcations in the bronchial tree. *Respir. Physiol.* 107:85-98.

Raabe, O.G., Yeh, H.C., Schum, G.M., and Phalen, R.F. 1976. *Tracheobronchial geometry: human, dog, rat, hamster*. Lovelace Foundation Report LF-53. Lovelace Foundation, Albuquerque, NM.

Robinson, R.J., and Yu, C.P. 1999. Coagulation of cigarette smoke particles. *J. Aerosol Sci.* 30:533-548.

Robinson, R.J., and Yu, C.P. 2001. Deposition of cigaertte smoke particles in the human respiratory tract. *Aerosol Sci. Technol*. 34:202-215.

Schiller, C.F., Gebhart, J., Heyder, J., Rudolf, G., and Stahlhofen, W. 1986. Factors influencing total deposition of ultrafine aerosol particles in the human respiratory tract. *J. Aerosol Sci.* 17:328-332.

Schiller, C.F., Gebhart, J., Heyder, J., Rudolf, G., and Stahlhofen, W. 1988. Deposition of monodisperse insoluble aerosol particles in the 0.005 to 0.2 μm size range within the human respiratory tract. *Ann. Occup. Hyg.* 32, Suppl. 1:41-49.

Schmid, O., Karg, E., Hagen, D.E., Whitefield, P.D., and Ferron, G. 2007, On the effective density of non-spherical particles from combined measurements of aerodynamic and mobility equivalent size. *J. Aerosol Sci*. 38:431-443.

Schroeter, J.D., Musante, C.J., Hwang, D., Burton, R., Guilmette, R., and Martonen, T.B. 2001. Hygroscopic growth and deposition of inhaled secondary cigarette smoke in human nasal pathways. *Aerosol Sci. Technol.* 34:137-143.

Schum, G.M., and Yeh, H.C. 1980. Theoretical evaluation of aerosol deposition in anatomical models of mammalian lung airways. *Bull. Math. Biol.* 41:1-15.

Slowik, J.G., Stainken, K., Davidovits, P., Williams, L.R., Jayne, J.T., Kolb, C.E., Worsnop, D.R., Rudich, Y., DeCarlo, P.F., and Jimenez, J.L. 2004. Particle morphology and density characterization by combined mobility and aerodynamic diameter measurements. Part 2: Application or combustion-generated soot aerosols as a function of fuel equivalence ratio. *Aerosol Sci. Technol*. 38:1206-1222.

Wang, C.S., and Friedlander, S.K. 2007. Determination of surface area and volume of nanoparticle aggregates deposited in the human respiratory tract. *J. Aerosol Sci*. 38:980-987.

Yeh, H.C., and Schum, G.M. 1980. Models of human lung airways and their application to inhaled particle deposition. *Bull. Math. Biophys.* 42,:461-480.

Yu, C.P. 1985. Theories of electrostatic lung deposition of inhaled aerosols. *Ann. Occup. Hyg.* 29:219-227.

Yu, C.P., and Xu, G.B. 1986. Predictive models for deposition of diesel exhaust particulates in human and rat lungs. *Aerosol Sci. Technol.* 5:337-347.

FIGURE CAPTIONS

Figure 1 Comparison of theoretical predictions of total deposition with experimental data in human test subjects for a constant flow rate (Q) of 250 ml s^{-1}, but variable tidal volumes (TV) and breathing frequencies (Schiller et al., 1988).

Figure 2 Relationship between count median diameter (CMD) and total deposition in 14 human volunteers inhaling petrol, diesel and ETS aerosols.

Figure 3 Comparison of computed total deposition for polydisperse, spherical particles, based on individual breathing conditions and size distributions, and measured average total deposition in 14 volunteers plotted as a function of the volume-equivalent or thermodynamic particle diameter. In case of the experimental data, the plotted diameter is the mobility-equivalent particle diameter recorded by the SMPS. Model predictions considering the dynamic shape factor function obtained by fitting the experimental data of Park et al. (2004) and Slowik et al. (2004) relate the measured mobility-equivalent diameters to the corresponding volume-equivalent diameters used in the model simulations.

Figure 4 Comparison of measured average fractional deposition with theoretical predictions for monodisperse, spherical particles using standard breathing conditions, plotted as a function of the volume-equivalent or thermodynamic particle diameter. In case of the experimental data, it was assumed that the particle diameter recorded by the SMPS represents the thermodynamic diameter.

Figure 5 Dynamic shape factor function for diesel aerosols obtained by fitting the experimental data of Park et al. (2004) and Slowik et al. (2004).

Table 1

Anatomical and respiratory parameters of 6 female (f) and 8 male (m) nonsmoking human volunteers derived from pulmonary function tests, grouped by gender and increasing FRC: Functional residual capacity (FRC), tidal volume (V_T), and breathing frequency (f).

Subject	Gender	FRC (l)	V_T (l)	f (min^{-1})
1	f	2.46	0.46	14
2	f	2.57	0.54	16
3	f	2.66	0.54	12
4	f	2.67	0.53	16
5	f	2.85	0.57	16
6	f	3.68	0.81	16
7	m	2.63	0.56	20
8	m	3.03	0.65	22
9	m	3.26	0.72	18
10	m	3.37	0.76	18
11	m	3.39	0.77	11
12	m	3.40	0.74	18
13	m	3.42	0.80	12
14	m	3.79	0.89	20
Average		3.08 (2.99)*	0.67 (0.61)*	16 (13)*

*standard ICRP (1994) values (average of male and female values)

Table 2

Count median diameters (CMD) with geometric standard deviations (GSD) of the petrol, diesel and ETS aerosols used in each deposition experiment for a specific volunteer and corresponding model predictions of total deposition (TD) for nasal breathing conditions, using subject-specific lung volumes and respiratory parameters.

	Petrol			Diesel			ETS		
Subject	CMD (nm)	GSD	TD (%)	CMD (nm)	GSD	TD (%)	CMD (nm)	GSD	TD (%)
1	62	1.8	35.9	122	1.8	23.8	177	1.7	18.1
2	63	1.7	36.0	124	1.7	23.1	217	1.7	16.1
3	63	1.6	38.6	139	1.8	23.8	177	1.7	20.3
4	70	1.8	33.0	100	1.8	26.0	153	1.8	20.1
5	76	1.6	31.2	138	1.9	22.2	190	1.7	17.5
6	72	1.8	33.3	146	1.9	21.7	210	1.7	17.7
7	87	1.8	27.3	97	1.9	25.7	156	1.6	18.1
8	57	1.6	34.4	100	1.8	24.4	134	1.7	20.0
9	59	1.6	36.0	128	1.7	21.7	224	1.6	15.6
10	117	1.8	23.7	187	1.8	18.4	196	1.7	17.3
11	64	1.8	40.7	127	1.8	26.8	205	1.7	19.8
12	60	1.7	35.8	126	1.8	22.6	212	1.7	16.3
13	73	1.7	36.6	111	1.8	28.4	174	1.8	21.5
14	43	1.7	41.9	87	1.8	28.0	130	1.7	20.9
Average	69.0	1.7	34.6 (± 4.8)	123.7	1.8	24.0 (± 2.7)	182.5	1.7	18.5 (± 1.9)

Table 3

Comparison of different modeling assumptions on particle deposition. Standard breathing refers to an FRC of 3300 ml and ICRP (1994) sitting breathing conditions, while individual breathing refers to the measured anatomical and physiological parameters (FRC, V_T, f) for each volunteer.

Inhalation conditions	Average total deposition (%) Petrol	Diesel	ETS
Monodisperse, average CMD standard breathing	42.7	29.6	22.0
Polydisperse, average CMD standard breathing	34.9	24.6	18.8
Polydisperse, average CMD individual breathing	33.8	23.5	18.3
Monodisperse, individual CMD individual breathing	42.4	29.2	21.2
Polydisperse, individual CMD individual breathing	34.6	24.0	18.5

Table 4

Comparison between experimental data and theoretical predictions for the three test aerosols.

		Total deposition (%)		
		Petrol	Diesel	ETS
Experiment	male	43.0	30.5	37.0
	female	39.2	28.3	35.2
	total	41.4	29.6	36.2
Model	male	34.9	24.5	18.7
	female	34.1	23.3	18.2
	total	34.6	24.0	18.5

Table 5

Empirical average dynamic shape factors, defined as the ratio of the CMDs measured in the experiments (CMD) divided by the CMDs of the reduced hypothetical size distributions to match the corresponding experimental values (CMD*).

Aerosol	CMD (nm)	CMD*(nm)	
Petrol	69	57	1.21
Diesel	124	78	1.59
ETS	183	68	2.69

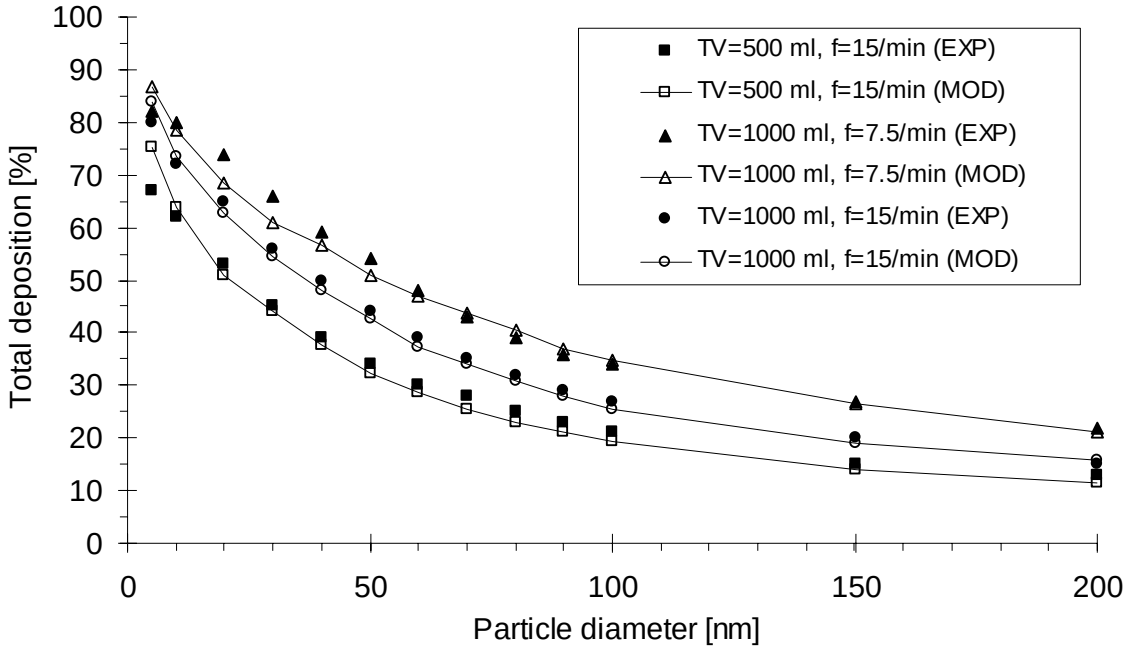
Total deposition [%]
Particle diameter [nm]
0
10
20
30
40
50
60
70
80
90
100
0
50
100
150
200
TV=500 ml, f=15/min (EXP)
TV=500 ml, f=15/min (MOD)
TV=1000 ml, f=7.5/min (EXP)
TV=1000 ml, f=7.5/min (MOD)
TV=1000 ml, f=15/min (EXP)
TV=1000 ml, f=15/min (MOD)

Figure 1

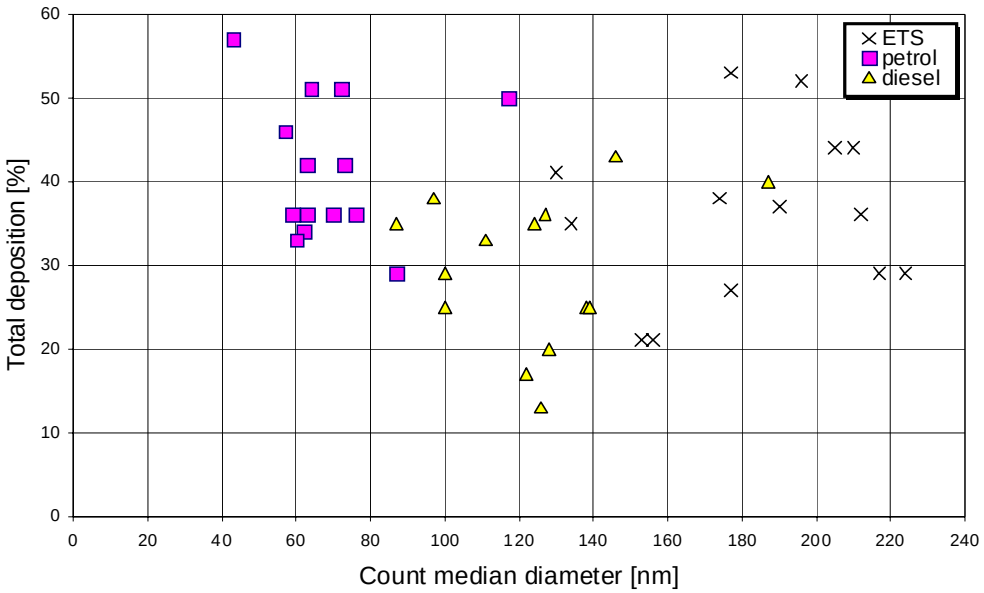
Total deposition [%]
Count median diameter [nm]
ETS
petrol
diesel
0
10
20
30
40
50
60
0
20
40
60
80
100
120
140
160
180
200
220
240

Figure 2

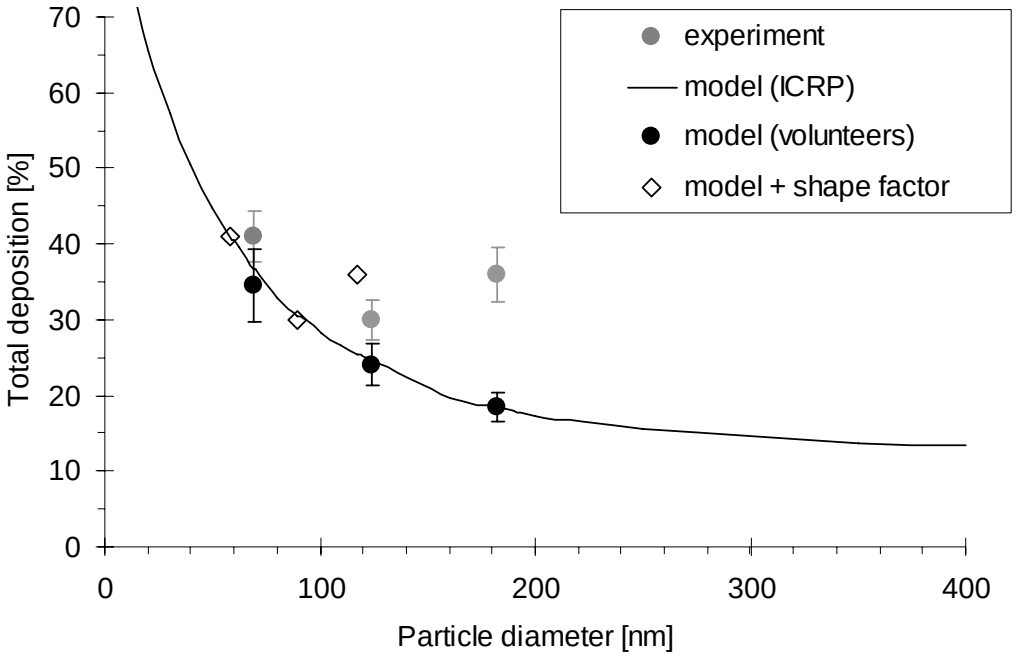
70
60
50
40
30
20
10
0
Total deposition [%]
0
100
200
300
400
Particle diameter [nm]
experiment
model (ICRP)
model (volunteers)
model + shape factor

Figure 3

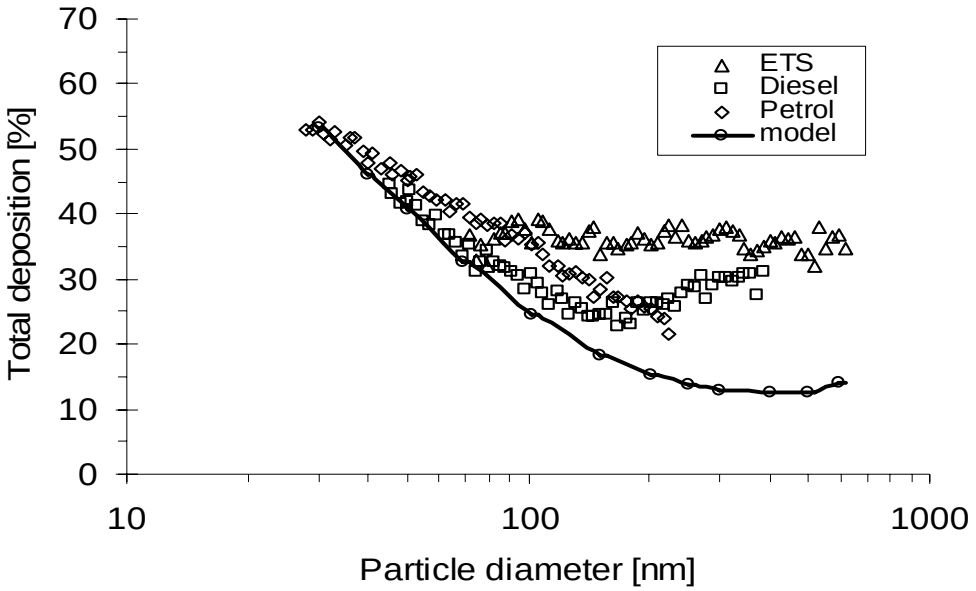
70
60
50
40
30
20
10
0
Total deposition [%]
10
100
1000
Particle diameter [nm]
ETS
Diesel
Petrol
model

Figure 4

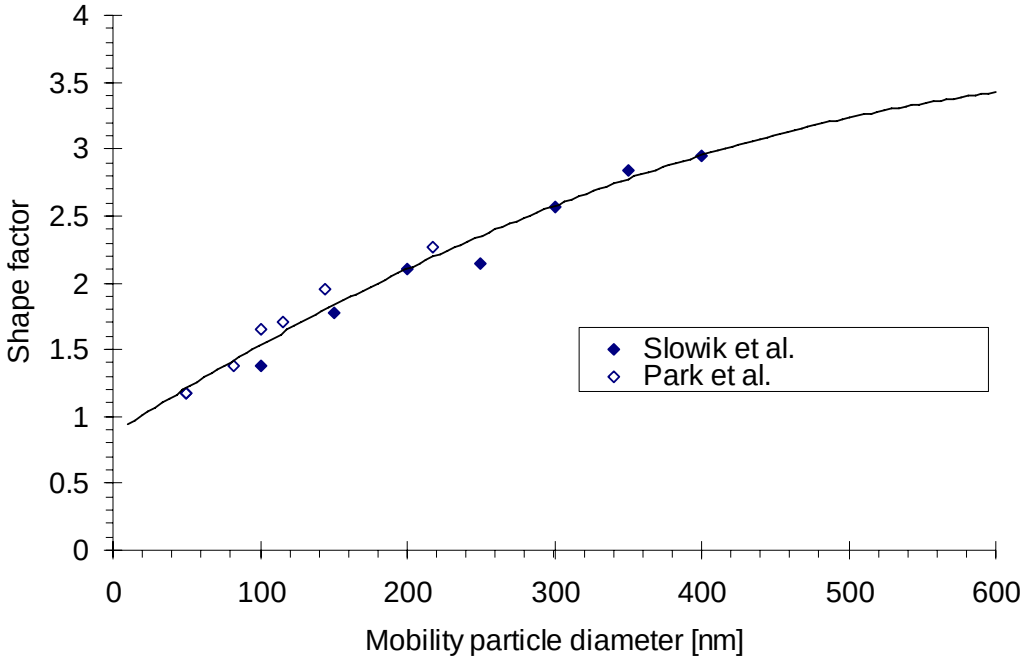
Shape factor
Mobility particle diameter [nm]
0
0.5
1
1.5
2
2.5
3
3.5
4
0
100
200
300
400
500
600
Slowik et al.
Park et al.

Figure 5